J Mol Model (2007) 13:1123–1131
DOI 10.1007/s00894-007-0231-6

ORIGINAL PAPER

Theoretical study on binding of S100B protein

Artur Gieldon · Mattia Mori · Rebecca Del Conte

Received: 27 March 2007 / Accepted: 29 June 2007 / Published online: 23 August 2007

Abstract S100B protein is one of the factors involved in the down-regulation of tumor suppressor protein p53, a transcription activator that signals for cycle arrest and apoptosis. As the inactivation of normal p53 functions is found in over half of human cancers, restoration of normal p53 functions through the destruction or prevention of S100B - p53 complexes represents a possible approach for the development of anti-cancer drugs. The aim of this work was to propose the S100B binding interface through an examination of the literature and use of molecular modeling (MM) techniques with AutoDock program and the AMBER force field. We propose two residues in the S100B binding pocket (Val56, Phe76) and two residues on the protein surface (Val52, Ala83) are essential for ligand binding. The data presented here indicate that interactions with these four residues are necessary for a reduction in the incidence of the S100B - p53 complex. Additionally, we have tried to explain a mechanism for the action of pentamidine, the best-known S100B ligand, and have proposed two S100B - pentamidine structures. The results presented here may be useful for the efficient design of new S100B ligands.

A. Gieldon · M. Mori · R. Del Conte
Protera S. r. l.,
Viale delle Idee, 22,
50019 Sesto Fiorentino (Fi), Italy

A. Gieldon (✉)
Institute of Biochemistry, Johan Wolfgang Goethe University,
Max-von-Laue-Str. 7,
60438 Frankfurt a.M., Germany
e-mail: gieldon@proterasrl.com

Keywords AMBER · AutoDock · Pentamidine · p53 · S100B · TRTK-12

Introduction

S100B is a member of a small (25 members at present) EF-hand calcium-binding protein family with molecular weights ranging from 10 to 12 kDa [1, 2]. The family was called S100 because the first known member (S100B) was soluble in a 100% ammonium sulphate saturated solution [3]. Members of the S100 family share high sequence and structural homology (25–65%) [2, 4]. The protein core consists of four helices (H1–H4) connected by loops. The loops between H1 - H2 and H3 - H4 and a portion of the connected helices contain the EF-hand calcium-binding motifs. The H2 - H3 loop is very important for the biological function of the protein, and is called the "hinge" [5]. All members of the S100 family exist in homodimeric or heterodimeric complexes with a predominance of homodimers; in this work S100B was considered to be a homodimer. The literature indicates that dimerization is very important for the biological function of members of the S100 family [1, 6].

S100B is one of the most well-characterized proteins of the S100 family. It is involved in the regulation of many cellular processes (e.g., energy metabolism [7, 8] and the cell cycle [9]), but the molecular mechanisms controlling its activity are not fully understood. Elevated levels of S100B have been observed in patients with brain injuries [10] and neurological diseases [11, 12] such as Creutzfeldt - Jakob and Alzheimer's [13]. Higher levels of S100B are also associated with the neurodegenerative lesions observed in patients with Down syndrome [14]. In addition, S100B is known to be a marker for several types of cancers [15–17].

S100B is one of the factors involved in the down-regulation of tumor suppressor protein p53 [1, 5, 18, 19], a transcription activator that signals for cell cycle arrest and apoptosis, and plays a pivotal role in the maintenance and regulation of normal cellular functions. Inactivation of p53 affects cell cycle checkpoints, apoptosis, gene amplification, and centrosome duplication [20, 21]. The cellular functions of p53 are controlled by the creation and destruction of the S100B-p53 complex [22, 23]. Mutational inactivation of the p53 coding gene (TP53) is detected in more than half of human cancers [20, 24–26]. Therefore, the inhibition of S100B-p53 interactions and restoration of normal p53 functions represents a possible approach for developing a cure for those cancers associated with elevated levels of S100B [1, 27].

S100B interacts with TRTK-12 (TRTKIDWNKILS), a synthetic peptide that was identified through the screening of a bacteriophage random peptide display library [28]. Binding of TRTK-12 to S100B blocks the S100B mediated inhibition of GFAP assembly [29, 30] and interactions with cytoskeletal proteins [31]. Experimental data have confirmed that full-length p53 binds to a site on S100B that overlaps the TRTK-12 peptide-binding site [2, 32]. The same conclusions were made by Garbuglia et al. [33] with regard to the S100A1 protein.

Literature review

S100B model

For modeling and structural analysis three (Ca^{2+} loaded) S100B structures were selected: 1MWN [34] (rat, S100B - TRTK-12 complex), 1MQ1 [35, 36] (synthetic human, S100B - TRTK-12 complex) and 1DT7 [37] (rat, S100B-p53 fragment). Human and rat S100B proteins share high sequence similarity, with only two differences, in the positions 62 N/E and 78 A/S (in human/rat, respectively). The bovine (1PSB [38]) model was not chosen, because of a mutation in the residue at position 80 (V/I in human/bovine), which plays a role in p53/ligand binding to S100B protein [37]. The rabbit (1JWD [39]) structure was rejected for the same reason (the difference in position 73, F/Y in human/rabbit, respectively).

Each of the three selected S100B models also share high structural similarity: the root mean square deviation (RMSD) between human and rat is 4.4 Å, and between two rat models is 2.2 Å [40].

The most significant differences between human and rat structures were observed in the hinge region (the loop between H2 and H3) and in H4. In the human, the C-terminal region of H4 is rotated counter-clockwise and pushed outside of the protein core with respect to the rat structures (the distance between the C^{α} of Ala6 in H1 and His85 in H4 is 16.9/15.4 Å in human/rat, respectively). Two selected rat structures share high structural identity (the backbone trace and side-chain conformations are similar, even though S100B is bound to different compounds, i.e., TRTK-12 (1MWN) and p53 fragment (1DT7), and differs in the presented regions from S100B (1MQ1) human protein. There are no significant structural differences in the remainder of S100B.

In the hinge loop, the most conformational diversity is exhibited at the residues: Ser41, Phe43, Leu44, and Glu46. In 1MQ1 (human), interactions between the ligand and residues: Ser41, Phe43, and Leu44 are not possible because the side-chains face toward the outside of S100B, to the contrary of rat protein in which those residues are directed toward the inside of the protein. The same situation can be observed in rat protein regarding Glu46 conformation, the side-chain of which is directed toward the outside/inside of rat/human proteins, respectively. The other important residue in the hinge loop, Glu45, has a similar conformation in all analyzed S100B structures, and is directed toward the inside of the protein. A detailed hinge loop analysis shows that His42 and Glu45 in human and rat S100B and Glu46 only in rat protein can all accommodate two conformations (i.e., point toward the inside or the outside).

Three conclusions were drawn from the presented data. First, the conformation of the hinge loop and, indeed, the entire S100B protein, is similar when complexed with TRTK-12 or p53 (according to available rat structures). Second, the structure of human S100B when bound to p53 protein will probably be more similar to the 1MQ1 structure than to the 1DT7 (to date, human S100B-p53 structure is unknown). Third, the hinge loop is highly flexible and adaptable to newly bound ligands.

S100B-TRTK-12 binding interface

[In all protein - ligand interface descriptions the following convention was used: a three-letter abbreviation for a protein residue and one-letter code for a ligand.]

[A in-house tool was used for the interaction analysis. If the distance between the closest atoms (except hydrogen) from selected residues was less than 4.1 Å, the interaction was identified.]

As mentioned before, two S100B - TRTK-12 complexes were considered in this work: 1MWN (rat) [34] and 1MQ1 (human) [36]. These structures differ greatly (in the TRTK-12 binding mode) and may be briefly described as horizontal - human and vertical - rat. (see Figs. 1a and c). All interactions are summarized in Schemes 1a and c and in Table 1.

An analysis of the S100B - TRTK-12 human structure indicates the presence of three complex-stabilizing interac-

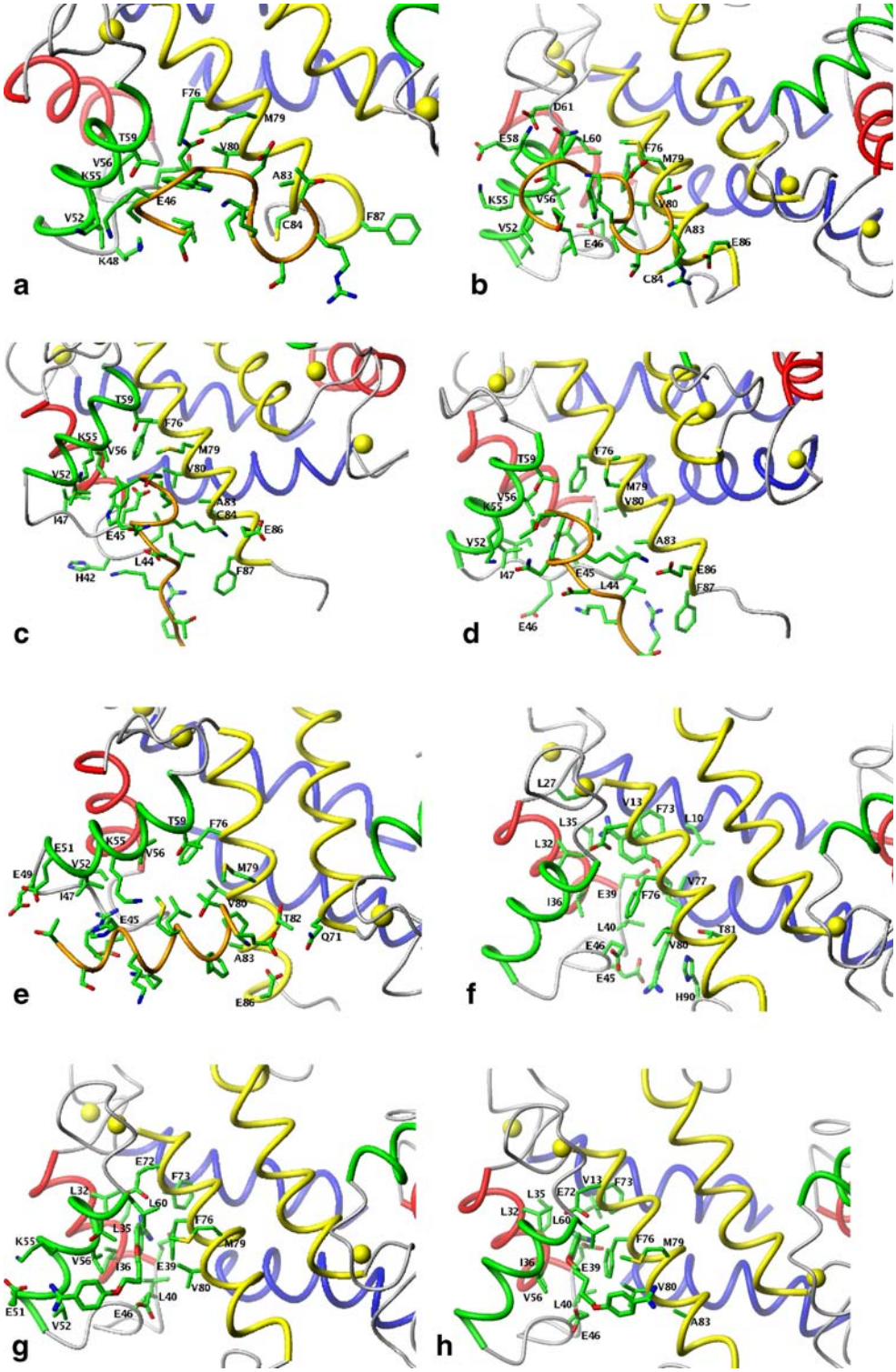

Fig. 1 **a**: S100B - TRTK-12, 1MQ1 structure [36]. **b**: S100B - TRTK-12, 1MQ1 modified structure. **c**: S100B - TRTK-12, 1MWN structure [34]. **d**: S100B - TRTK-12, 1MWN modified structure. **e**: S100B - p53, 1DT7 structure [37]. **f**: S100B - pentamidine (SBi1) (AMBER) - lit. structure [52]. **g**: S100B - pentamidine (SBi1) (AMBER). **h**: S100B - pentamidine (SBi1) (AutoDock)

tion networks. The N-terminal region of TRTK-12 is involved in the hydrogen bond network contributed to by T1, R2, Glu86 and Gln71 from the second S100B monomer. In the middle, a large hydrophobic cluster with W7 at the center, and I5, I10, L11 on the peptide side (bottom) and Val56, Phe76, and Val80 on the protein side (top) is present. At the C-terminal region, hydrophobic contacts between I10 and Val52, Val56 and alkyl chains

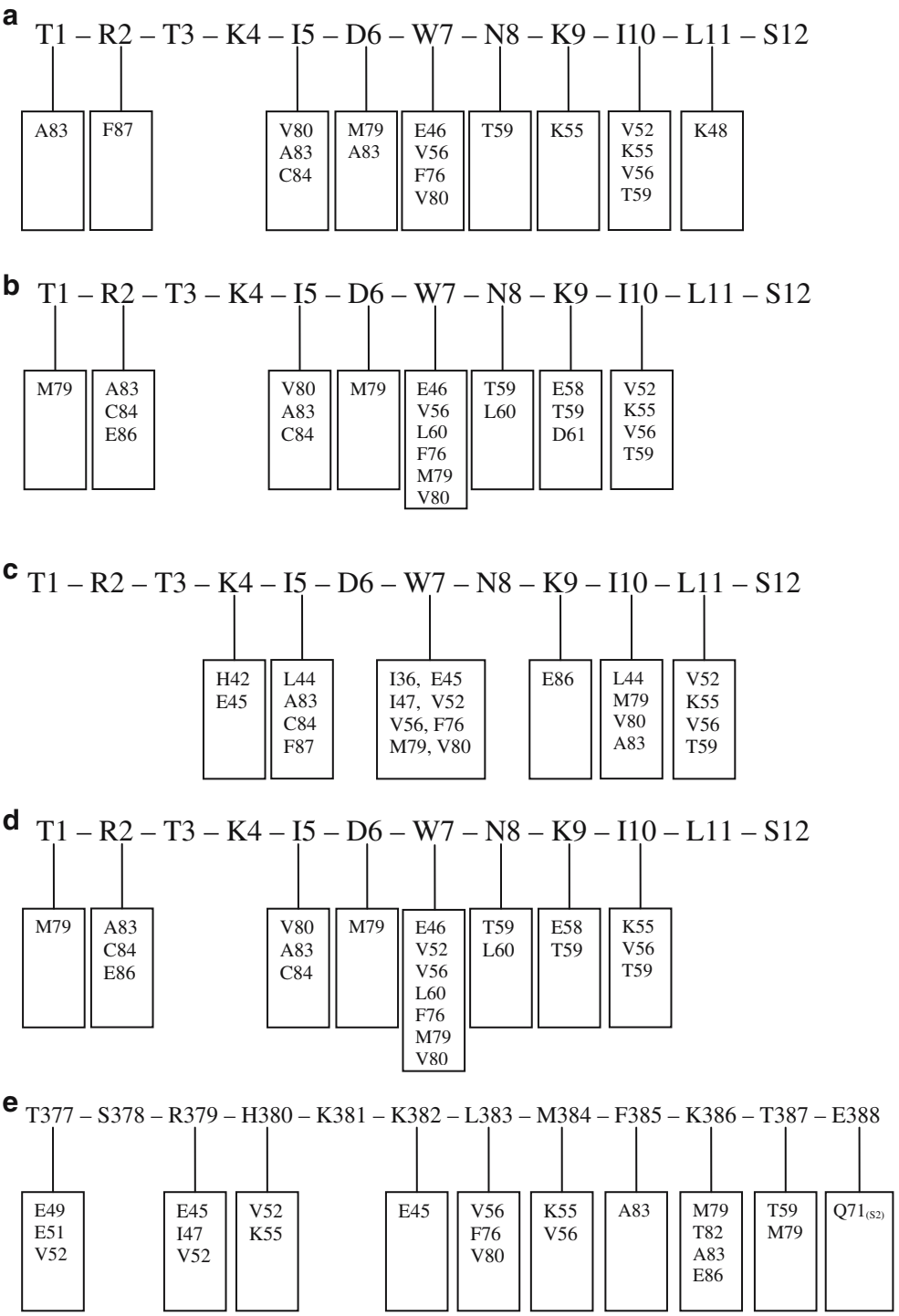

Scheme 1 **a**: Side-chain - side-chain interface interactions: S100B - TRTK-12, 1MQ1 structure [36]. **b**: Side-chain - side-chain interface interactions: S100B - TRTK-12, modified 1MQ1 structure. **c**: Side-chain - side-chain interface interactions: S100B - TRTK-12, 1MWN structure [34]. **d**: Side-chain - side-chain interface interactions: S100B - TRTK-12, modified 1MWN structure. **e**: Side-chain - side-chain interface interactions: S100B - p53 peptide, 1DT7 structure [37]

interaction between K9 and Lys55 are seen (the charged amine groups are opposed) (see Scheme and Fig. 1a).

The S100B - TRTK-12 rat complex differs greatly from the human one. The N-terminal region of TRTK-12 is not associated with the interaction, instead a Glu46 - K4 salt bridge and a hydrophobic cluster involving I5, I10 and Ala83, Phe87 are found. Likewise, in the human S100B - TRTK-12 complex, a large hydrophobic cluster with W7 at the center is present. In this case, W7 is surrounded by L11 and Val52, Phe76 and Glu45. W7 and Glu45 side-chains are located parallel to one another in the immediate vicinity. The final interaction is a presumed salt bridge between K9 and Glu86 (Glu86 carboxyl and K9 amine groups are opposed) (see Scheme and Fig. 1c).

Table 1 S100B interface residues identified after structural analysis

S100B	H1 (1–17)	L1 (18–28)	H2 (29–39)	L2 (40–49)	H3 (50–60)	L3 (61–69)	H4 (70–87)	L4 (88–91)
TRTK-12 [1MWN] [34]			I36,	H42, L44, E45, I47,	V52, K55, V56, T59,		F76, M79, V80, A83, C84, E86, F87,	
TRTK-12 [1MQ1] [36]				E46, K48,	V52, K55, V56, T59,		F76, M79, V80, A83, C84, F87,	
p53 [1DT7] [37]				E45, I47, E49,	E51, V52, K55, V56, T59,		F76, M79, V80, T82, A83, E86, $Q71_{(S2)}$,	
TRTK-12 [1MWN] - mod.				L44, E45, E46, I47,	V52, K55, V56, T59,		F76, M79, V80, A83, F87,	
TRTK-12 [1MQ1] - mod.				E46,	V52, K55, V56, E58, T59, L60,	D61,	F76, M79, V80, A83, C84, E86,	
SBi1 AMBER			L32, L35, I36, E39,	L40, E46,	E51, V52, K55, V56, T59, L60,		E72, F73, F76, M79, V80,	
SBi1 AUTODOCK	V13,		L32, L35, I36, E39,	L40, E46,	V56, L60,		E72, F73, F76, M79, V80, A83	
SBi1 – lit. [52]	L10, V13,	L27,	L32, L35, I36, E39,	L40, E45, E46,			E72, F73, F76, V77, V80, T81,	H90,

In the brackets, literature references and pdb structure names are given.

Despite these differences, both structures share a common core mechanism with the W7 residue in the center. The importance of W7 has been confirmed experimentally [5, 32, 34, 36, 41].

S100B - p53 binding interface

The conformation of the p53 fragment (SHLKSKKGQS **TSRHKKLMFKTE**; residues marked bold are shown in Fig. 1e as being involved in the S100B - p53 peptide interface) present in the 1DT7 [37] pdb structure can be described as horizontal, similar to the arrangement of TRTK-12 in human (1MQ1) [36] S100B (see Fig. 1e). Contrary to TRTK-12, in the 1MQ1 pdb structure the N-terminal region of the p53 peptide in the 1DT7 model is placed near H3. All S100B - p53 peptide fragment contacts are summarized in Table 1 and Scheme 1e. The most important interaction with H3 appears to be the network of hydrogen bonds between T377 and Glu49 and Glu51. The most significant interaction with the hinge loop is the salt bridge between R379 and Glu45 [32]. L383, Val56 and Phe76 constitute the core interaction. Two interactions were found at the C-terminal region of p53 fragment; the salt bridge between K386 and Glu86 and the hydrogen bond between E388 and Gln71 from the second monomer (see Fig. and Scheme 1e). Almost all of the S100B - p53 peptide interface residues were marked by HSQC [5, 47] and NOESY [37] experiments (see Table 2). From H3, Glu51 was barely detectable but Glu49 was not. The Glu86 - K386 salt bridge, clearly visible from the structure, was well detectable experimentally [5, 32]. Detailed structure analysis indicates that some of the residues with high chemical shifts do not belong to the S100B - p53 peptide interface. For example, Val53 is involved in the H2 - H3 interaction and

Table 2 S100B residues with high chemical shift perturbations

S100B	H1 (1–17)	L1 (18–28)	H2 (29–39)	L2 (40–49)	H3 (50–60)	L3 (61–69)	H4 (70–87)	L4 (88–91)
Pentamidine (SBi1) [52]	A9, I11, F14, H15,			S41, F43, L44, E45, E46,	V52, D54, T59, L60,		M74, A75, V77, A83,	F88, E89, H90, E91,
p53 [1DT7] [47]	L3, D12, F14,		I36,	S41, F43, L44, E45, E46, I47, K48,	V52, V53, D54, V56, T59,	D61, N62,	A75, F76, V77, A78, M79, V80, T81, T82, A83, C84, H85, E86, F87,	F88, H90,
TRTK-12 [1MQ1] [41]	S1, E2, A6, V13, F14, Y17,	S18, G19, H25, L27,	K29, E31, E34, L35, N37, N38,	S41, H42, I47, E49,	E51, V52, V53, V56,	D63, G64, C68, D69,	F70, E72, F73, V77, A83, C84, F87,	F88,

In the brackets, literature references and pdb structure names are given.

Thr81 and Phe88 are involved in the H1 - H4 interaction. We may speculate that these chemical shifts are caused by an internal conformational change of S100B protein after p53 peptide binding as proposed in [32].

Analysis of the literature chemical shift perturbations in the context of available pdb structures

Structural analysis indicates that residues with high chemical shift perturbations as identified by NMR experiment can be divided into two groups: residues on the S100B - ligand interface and residues involved in the S100B conformational changes as postulated in [32]. (All available data from the literature are summarized in Table 2.)

In the S100B - p53 1DT7 pdb structure [37], several residues were identified as potentially involved in the S100B conformational change. Interactions between Ser78 - Ser78 and Ala75 - Ser78 are potentially involved in conformational change between helix four (H4 - H4) from the first and second (second and first) monomer. A similar role can be assigned to the Leu3 - Val77 interaction. A weak salt bridge or hydrogen bond dependent on histidine conformation was found between Asp12 and His90. Thr81 and Thr82 are also potentially involved in H4 - H4 interaction, but the second residue for interaction (Met74) was not detected with NMR [5, 37]. Two residues with high chemical shift perturbations (Asp61 and Asn62) are placed at the second EF-hand calcium-binding motif and are probably involved in the protein conformational change. We also identified a large network of hydrophobic interactions on one side of the S100B binding pocket, on the helix 3 (H3), with the following residues involved in the conformational change of S100B: I36, I47, V52, V53, and V56. In the S100B - TRTK-12 1MQ1 structure [36, 41] we identified only two residue pairs with potential involvement in the S100B conformational change: Ala6 - Ala6 and Val13 - Leu35 between two and within one monomer, respectively. Additionally, Phe70 was putatively identified as responsible for the H4 - H4 conformational change. High chemical shift perturbations were observed in three residues (Ser18, Leu27, Glu31) at the first EF-hand calcium-binding motif, and five residues (Asp63, Gly64, Cys68, Asp69, and Glu72) at the second [36, 41]. The hydrophobic interactions identified in the 1DT7 structure also exist and all residues (except Ile36) are detectible with NMR.

From experiment to hypothesis

Methods

Molecular modeling (MM) techniques and AMBER v. 7.0 force field [42] were used to simulate the described systems (rat and human S100B - TRTK-12 structures and S100B (1MQ1) - pentamidine complexes). All complexes were minimized and simulated using very short (3 ps) and low temperature (50 K) molecular dynamics (MD). Time step was set as 0.1 fs and the non-bonding parameters were updated every 10 steps. Calculations were carried out *in vacuo* with a partial compensation for environmental interactions made by setting the dielectric permeability ε equal to 4R. During the simulation, positional constraints on all C^{α} atoms were applied. The preceding protocol was used as a consequence of the assumption to maintain the shape of the structure as much as possible while observing side-chain adaptations. Large time scale molecular dynamics with an explicit environment would have greatly widened the search area on the hypersurface of potential energy, and most probably would have located a minimum value far away from the experimental structure. However, with significant structural differences (between computed and experimental) it would be impossible to validate the obtained results. Additionally, S100B binding affinities are strongly connected with minor conformational change of the protein (see next section).

For the ligand docking (see S100B - pentamidine (SBi1) binding model), the AutoDock v. 3.0 [43] program with an implemented genetic algorithm was used. A 25×25×30 Å docking space (enough to cover one monomer) and 0.25 Å grid point were applied. Initial ligand coordinates were set at random. Fifty individuals in the population and 37000 generations were used as genetic algorithm parameters. Three hundred iterations of a Solis & Wets local search were applied as implemented in AutoDock [43]. The lowest energy conformation is presented on Fig. 1h.

Modified S100B - TRTK-12 binding model

The addition of Ca^{2+} to apo-S100B causes a large conformational change in helix 3 (H3) [44–46]; it rotates ~90° and the H3 - H4 intrahelical angle changes by 60 degrees. As a consequence, S100B switches from a “closed” to an “open” conformation. The addition of p53 indicates a minor change in the angle between helices (4°±4°, with the error equal to the value of the variation) [37]. This 4 degrees change in intrahelical angle may not seem important but our study shows that this minor self-adaptation of S100B is significant and may play a key role in ligand binding. Self-adaptation of S100B protein for binding of the p53 peptide fragment was observed by Markowitz et al. [47] (see Fig. 1e). Experimental data indicate that after the binding of the p53 peptide fragment, the S100B structure becomes more rigid [34, 37, 48].

As mentioned before, a review of the literature has led us to conclude that the S100B binding core takes the place of the TRTK-12 peptide, W7 side-chain interaction. Val56

(H3) and Phe76 (H4) constitute a hydrophobic entrance to the S100B binding pocket. Phe76 appears to play an important role, because it can make a sandwich-like interaction with the potential ligand. An appropriate distance between Val56 and Phe76 (C^{α}-C^{α}, 8.2, 9.7, and 9.3 Å in 1MWN, 1MQ1, and 1DT7, respectively) seems to be critical for this interaction to occur. In 1MQ1, a typical sandwich-like interaction is possible, as the second ring can fit between Val56 and Phe76. With some difficulty, it will also fit in the 1DT7 structure, but a sterical snag in 1MWN makes this type of interaction impossible to occur. For the sake of comparison, analysis of the proposed hydrophobic entrance was performed on two additional models: 1UWO [49] (NMR, apo-S100B, human structure) and 1XYD [48] (NMR, holo-S100B, zinc and calcium bound rat structure). The value of C^{α}-C^{α} distance between Val56 and Phe76 was 6.6 Å and 8.0 Å in 1UWO and 1XYD, respectively.

In both computed models, the position of the TRTK-12 peptide was adjusted to facilitate a "sandwich-like" interaction between W7 and Phe76. In order to maximally maintain the shape of the structure, the changes applied in both cases were minor. The (2.5; −3.5; 1.5) and (3.0; −6.0; −2.0) [Å] translation and (0.0; 0.0; 7.0) and (0.0; 0.0; 8.0) [degrees] rotation vectors were used to change the position of TRTK-12 peptide in the 1MQ1 and 1MWN structures, respectively. The goal was to ascertain if S100B and TRTK-12 in the modified conformation are mutually adaptable and if the W7 - Phe76 "sandwich-like" interaction is possible.

Modified S100B - TRTK-12 binding interface

Several putatively important interactions were identified in both of the modified S100B - TRTK-12 structures. At the N-terminal region of human TRTK-12 (see Fig. and Scheme 1b), interaction with the second monomer (Gln71) disappeared after MD, leaving only the R2 - Glu86 salt bridge. Contrarily, T1 developed a hydrogen bond with the Thr82 - Ala83 peptide bond, and a small hydrophobic cluster with I5 in the center and Val80 and Ala83 on both sides was formed. The most important interaction with W7 was also retained, but only Val56 and Phe76 on the protein side and I5 and L11 on the TRTK-12 side were involved. The W7 interaction received additional stabilization from a hydrogen bond with Glu46 from the hinge loop. All hydrophobic interactions between I10 and V52 and V56 were maintained, and additionally, I10 interacted with the Lys55 alkyl chain.

In the modified rat model (see Fig. and Scheme 1d) the I5-centered hydrophobic cluster was present, but in this case only two residues from the protein (Leu44 and Ala83) were involved. The core interaction with W7 in the center was present but in this case, instead of L11 from TRTK-12 peptide, I10 was involved. On the protein side, Val52 and Val56 were found. The W7 - Phe76 interaction was also found but the side-chain rings were placed serially in one plane. As in the human model, the hydrogen bond with the hinge loop residue was present, but in this case, Glu45 instead of Glu46 was involved.

S100B - pentamidine isothionate (SBi1) binding model

Pentamidine is a member of aromatic diamidines [50], currently in widespread clinical use for the treatment of *Pneumocystis carinii* pneumonia (PCP) [51]. Markowitz et al. [52, 53] proposed and tested pentamidine (referred in the literature as SBi1; isethionate salt was tested because it is approved by the FDA) for inhibition of the S100B - p53 interaction. Experimental results show that SBi1 binds to S100B at very low concentrations (~1 μM) [52, 53]. We therefore decided to combine the S100B - TRTK-12 binding model, knowledge about the structure of the S100B - p53 complex, and available experimental data [52] to determine a mechanism for this interaction. A modified 1MQ1 structure was selected for all simulations. Two computational protocols were used. In the first case the ligand was placed manually inside the S100B pocket and computed using AMBER v.7.0 forcefield [42] (50 K, 3 ps) as described before. In the second case the ligand was docked automatically with AutoDock v. 3.0 [43] program. According to our results pentamidine occurs in two conformations in the SBi1 - S100B complexes (see Fig. 1g and h). Including symmetry constraints, the number of "working" conformations is four. In both cases we identified identical sets of residues interacting with SBi1 in the S100B binding pocket (see Table 1). The differences were observed only on the protein surface, but in both cases the identified residues were also involved in p53 peptide binding [37]. This may provide an explanation for the good activity of pentamidine in the prevention or destruction of S100B - p53 interaction.

S100B - pentamidine isothionate (SBi1) binding interface

The most important interaction in the S100B binding pocket seems to be the hydrophobic one between pentamidine and Phe76 phenyl rings. We found also a putatively important salt bridge between SBi1 amidine group and Glu39 deep inside of the S100B binding pocket. The distance between the closest oxygen and nitrogen atoms was 2.9 Å. In both obtained complexes, the benzamidine group was surrounded by seven hydrophobic residues: Leu32, Ile36, and Val56 from helix 3 (H3), Phe76 and Val80 from helix 4 (H4), and two Leu40 and Leu60 from second (hinge) and third loops, respectively. Two binding sites were identified on the protein surface, depending on

the method used (see Figs. 1g and h). The first was found on the N-terminal region of H3 using molecular dynamics implemented in the AMBER v.7.0 package [42]. In this region the most important interactions seem to be the salt bridge between Glu51 and the SBi1 amidine group (the distance between the closest oxygen and nitrogen atoms was 3.0 Å) and the interaction with Val52. The second binding site was found to be in the middle part of H4 using AutoDock v. 3.0 program [43]. The SBi1 benzamidine group interaction with two residues: Val80 and Ala83 was observed in this region.

To facilitate comparison, the SBi1 - S100B complex in conformation described in [52] was build and modeled (see Fig. 1f). Pentamidine was placed vertically in the S100B binding pocket as seen in [52] and simulated in AMBER v. 7.0 force field [42]. In this case the first benzamidine group was surrounded by Leu10, Val13, Leu27, Leu35 and F73, which can form a hydrophobic "sandwich" similar to the "sandwich" described before. There was also the possibility of formation of a salt bridge between the amidine group and Glu72. The distance between the closest oxygen and nitrogen atoms was 4.3 Å. The second benzamidine group was placed near the hinge loop in the immediate vicinity of Leu40, Glu45, and Glu46. In this case there was a possibility for the formation of two salt bridges. The distances between the closest nitrogen atom from the amidine group and the oxygen atoms from Glu45 and Glu46 were 4.7 and 4.9 Å, respectively. From the C-terminal region of S100B the most important interaction seems to be that with His90. According to our results this S100B - pentamidine (SBi1) conformation cannot prevent p53 binding because there are no interactions with Val52 and Ala83 on the protein surface.

Discussion and conclusions

In this work we used data from the available literature and molecular modeling (MM) techniques to propose a ligand-binding mechanism for the S100B protein. As shown, the most important residues in the S100B binding pocket seems to be Val56 and Phe76 from the third (H3) and the fourth (H4) helices, respectively which constitute a hydrophobic entrance to the S100B binding pocket. We hypothesize that Phe76 can make a "sandwich-like" interaction with the potential ligand. The holo-S100B protein can adapt to the presence of a ligand through a minor change in the angle between H3 and H4. This was clearly visible in a comparison of the C^{α}-C^{α} distance between Val56 and Phe76 in several available holo-S100B structures. On the protein surface we identified two residues which were ubiquitous throughout the literature and in every performed simulation: Val52 and Ala83. As a detailed structure analysis indicated that these two residues cannot be involved in the S100B conformational change, we speculate that interaction with Val52 or Ala83, or both concurrently, is necessary for a prevention of p53 binding by S100B.

Using data available in the literature, we modeled the S100B - pentamidine (SBi1) interactions and found two potential conformations capable of preventing p53 binding to S100B. The presented models are in good agreement with available experimental data. Additionally, using detailed structure analysis we verified the residues responsible for ligand binding and those involved in the protein conformational change.

Acknowledgments We would like to thank professor Claudio Luchinat for all guidance and professor David Weber for a very inspiring discussion about S100B protein.

This work was supported by European Union Community, Marie Curie Host Fellowships for TOK, contract n. MTKI-CT-2004-509750.

References

1. Donato R (2001) In J Biochem Cell Biol 33:637–668
2. Santamaria-Kisiel L, Rintala-Dempsey AC, Shaw GS (2006) Biochem J 396:201–214
3. Moore BW (1965) Biochem Biophys Res Commun 19:739–744
4. Schafer BW, Heizmann CW (1996) TIBS 21:134–140
5. Rustandi RR, Drohat AC, Baldisseri DM, Wilder PT, Weber DJ (1998) Biochem 37:1951–1960
6. Ferguson PL, Shaw GS (2002) Biochem 41:3637–3646
7. Zimmer DB, Van Eldik LJ (1986) J Biol Chem 261:11424–11428
8. Landar A, Caddell G, Chessher J, Zimmer DB (1996) Cell Calcium 218:243–247
9. Millward TA, Heizmann CW, Schafer BW, Hemmings BA (1998) EMBO J 17:5913–5922
10. Rothermundt M, Peters M, Prehn JHM, Arolt V (2003) Microsc Res Tech 60:614–632
11. Heizmann CW (1999) Neurochem Res 24:1097–1100
12. Zimmer DB, Chaplin J, Baldwin A, Rast M (2005) Cell Mol Biol (Noisy-le-grand) 51:201–214
13. Krasnianski A, Meissner B, Schulz-Schaeffer W, Kallenberg K, Bartl M, Heinemann U, Varges D, Kretzschmar HA, Zerr I (2006) Arch Neurol 63:876–880
14. Netto CB, Portela LV, Ferreira CT, Kieling C, Matte U, Felix T, da Silveira TR, Souza DO, Goncalves CA, Giugliani R (2005) Clin Biochem 38:433–435
15. Torabian S, Kashani-Sabet M (2005) Curr Opin Oncol 17:167–171
16. Harpio R, Einarsson R (2004) Clin Biochem 37:512–518
17. Heizmann CW, Fritz G, Schafer BW (2002) Front Biosci 7:1356–1368
18. Cho Y, Gorina S, Philip DJ, Pavletich NP (1994) Science 265:346–355
19. Scotto C, Delphin C, Deloulme JC, Baudier J (1999) Mol Cell Biol 19:7168–7180
20. Hussain SP, Harris CC (2006) J Nippon Med Sch 73:54–64
21. Watson AJ (2006) Crit Rev Oncol Hematol 57:107–121
22. Lin J, Blake M, Tang C, Zimmer D, Rustandi RR, Weber DJ, Carrier F (2001) J Biol Chem 276:35037–35041
23. Lin J, Yang Q, Yan Z, Markowitaz J, Wilder PT, Carrier F, Weber DJ (2004) J Biol Chem 279:34071–34077

24. Hollstein M, Sidransky D, Vogelstein B, Harris CC (1991) Science 253:49–53
25. Matoba S, Kang JG, Patino WD, Wragg A, Boehm M, Gavrilova O, Hurley PJ, Bunz F, Hwang PM (2006) Science 312:1650–1653
26. Sun Y (2006) Mol Carcinog 45:409–415
27. Fernandez-Fernandez MR, Veprintsev DB, Fersht AR (2005) PNAS 102:4735–4740
28. Ivanenkov VV, Jamieson Jr GA, Gruenstein E, Dimlich RVW (1995) J Biol Chem 270:14651–14658
29. Bianchi R, Garbuglia M, Verzini M, Giambanco I, Ivanenkov VV, Dimlich RVW, Jamieson GA Jr (1996) Biochem Biophys Acta 1313:258–267
30. Frizzo JK, Tramontina F, Bortoli E, Gottfried C, Leal RB, Lengyel I, Donato R, Dunkley PR, Goncalves CA (2004) Neurochem Res 29:735–740
31. Frizzo JK, Tramontina AC, Tramontina F, Gottfried C, Leal RB, Donato R, Goncalves CA (2004) Cell Mol Neurobiol 24:833–840
32. Wilder PT, Lin J, Bair CL, Charpentier TH, Yang D, Liriano M, Varney KM, Lee A, Oppenheim AB, Adhya S, Carrier F, Weber DJ (2006) Biochim Biophys Act 11:1284–1297
33. Garbuglia M, Verzini M, Rustandi RR, Osterloh D, Weber DJ, Gerke V, Donato R (1999) Biochem Biophys Res Comm 254:36–41
34. Inman KG, Yang R, Rustandi RR, Miller KE, Baldisseri DM, Weber DJ (2002) J Mol Biol 324:1003–1014
35. McClintock KA, Shaw GS (2002) J Biomol NMR 23:255–256
36. McClintock KA, Shaw GS (2003) J Biol Chem 278:6251–6257
37. Rustandi RR, Baldisseri DM, Weber DJ (2000) Nature Struct Biol 7:570–574
38. Bhattacharya S, Large E, Heizmann CW, Hemmings B, Chazin WJ (2003) Biochem 42:14416–14426
39. Maler L, Sastry M, Chazin WJ (2002) Mol Biol 317:279–290
40. Ostendorp T, Heizmann CW, Kroneck PMH, Fritz G (2005) Acta Cryst F61:673–675
41. McClintock KA, Van Eldik LJ, Shaw GS (2002) Biochem 41:5421–5428
42. Pearlman DA, Case DA, Caldwell JW, Ross WS, Cheatham III TE, DeBolt S, Ferguson D, Seibel G, Kollman P (1995) Comp Phys Commun 91:1–41
43. Morris GM, Goodsell DS, Halliday RS, Huey R, Hart WE, Belew RK, Olson AJ (1998) J Comput Chem 19:1639–1662
44. Smith SP, Shaw GS (1998) Biochem Cell Biol 76:324–333
45. Maler L, Sastry M, Chazin WJ (2002) J Mol Biol 317:279–290
46. Weber DJ, Rustandi RR, Zimmer DB (2000) Interaction of dimeric S100B(ββ) with the tumor suppressor protein for Ca2+-dependent S100 target protein interactions. In: Pochet R (ed) Calcium: The molecular basis of calcium biology and medicine. Kluwer, Netherlands, pp 521–539
47. Markowitz J, Rustandi RR, Varney KM, Wilder PT, Udan R, Wu SL, Horrocks W, Weber DJ (2005) Biochem 44:7305–7314
48. Wilder PT, Varney KM, Weiss MB, Gitti RK, Weber DJ (2005) Biochem 44:5690–5702
49. Smith SP, Shaw GS (1998) Structure 6:211–222
50. Lowe PR, Sanson CE, Schwalbe CH, Stevens MFG (1989) J Chem Soc Chem Commun 16:1164–1165
51. Wispelwey B, Pearson RD (1991) Infect Control Hosp Epidemiol 12:375–381
52. Markowitz J, Chen I, Gitti R, Baldisseri DM, Pan Y, Udan R, Carrier F, MacKerell AD Jr, Weber DJ (2004) J Med Chem 47:5085–5093
53. Markowitz J, MacKerell AD Jr, Carrier F, Charpentier TH, Weber DJ (2005) Curr Top Med Chem 5:1093–1108